

## The effect of microtube formation with walls, containing Fe<sub>3</sub>O<sub>4</sub> nanoparticles, via gas-solution interface technique by hydrolysis of the FeCl<sub>2</sub> and FeCl<sub>3</sub> mixed solution with gaseous ammonia

V. E. Gurenko, V. P. Tolstoy, L. B. Gulina

Institute of Chemistry, Saint Petersburg State University,  
26 University Pr., St. Peterhof, Saint Petersburg, 198504, Russia

v.tolstoy@spbu.ru, l.gulina@spbu.ru, limeman14@gmail.com

PACS 75.70.Ak

DOI 10.17586/2220-8054-2017-8-4-471-475

In this work, microtubes with walls, containing Fe<sub>3</sub>O<sub>4</sub> nanoparticles, obtained by “rolling up” of the interfacial films, were synthesized by the gas-solution interface technique (GSIT), using a mixture of aqueous solutions of FeCl<sub>2</sub> and FeCl<sub>3</sub> and gaseous ammonia. The synthesized microtubes were characterized by Scanning Electronic Microscopy (SEM), Energy-Dispersive X-ray spectroscopy (EDX), X-Ray Diffraction analysis (XRD) and magnetization measurements. It was established that under optimal synthetic conditions the microtube diameter ranged from 5 to 10 μm, the length was up to 120 μm and the thickness of walls was about 0.6 μm, the walls themselves being formed by nanoparticles with a size of about 10 nm. The reversible hysteresis behavior, the low coercive force, the low remanence magnetization and the approaching of M<sub>r</sub>/M<sub>s</sub> to zero, confirmed the superparamagnetic nature of the synthesized microtubes. A hypothesis on the formation of microtubes by the gas-solution interface technique was proposed.

**Keywords:** Fe<sub>3</sub>O<sub>4</sub>, microtubes, magnetic behavior, superparamagnetic, Gas-Solution Interface, GSIT.

*Received:* 26 July 2017

*Revised:* 5 August 2017

### 1. Introduction

Iron oxides are known to be a significant class of inorganic compounds, which have great potential for practical application [1–8]. Among them, special attention is drawn to Fe<sub>3</sub>O<sub>4</sub> oxide with cubic crystal structure of magnetite and its unique magnetic, electrical and chemical properties [9–11]. These properties determine their possible application in the capacity of electrodes in lithium-ion batteries and sensors, wastewater treatment, and drug delivery. Therefore, a number of synthetic methods are used now, including precipitation of FeCl<sub>2</sub> and FeCl<sub>3</sub> mixture in an ammonium hydroxide solution [12].

Recently, much attention has been paid to the creation of hollow microparticles or, in a different terminology, microcapsules with walls formed by Fe<sub>3</sub>O<sub>4</sub> nanoparticles. These microcapsules have relatively high specific surface and can be applied in the creation of core-shell multifunctional nanostructures [13, 14]. Hollow Fe<sub>3</sub>O<sub>4</sub> microcapsules, for example, were obtained by hydrothermal method [15], one-pot solvothermal method using Fe(NO<sub>3</sub>)<sub>3</sub>·6H<sub>2</sub>O as the iron source, and glycerol, isopropyl alcohol (IPA) together with a small amount of water as a solvent [16], solvothermal method with template from surfactant micelles [17], and Ostwald ripening in magnetic field [18]. In such a case, the problem of synthesizing of the hollow microparticles with tubular morphology has a particular importance given that such microparticles will exhibit the unique combination of magnetic, optical and magneto-optical properties.

The aim of the present work was to investigate the possibility of obtaining microtubes with walls, containing Fe<sub>3</sub>O<sub>4</sub> nanoparticles, via GSIT as a result of the interfacial reaction between gaseous ammonia and a mixed solution of FeCl<sub>2</sub> and FeCl<sub>3</sub>.

The GSIT method was implemented for the synthesis of arsenic sulfide microtubes [19], manganese oxide [20, 21] and lanthanum fluoride [22–24]. A distinctive feature of this method is that, firstly, due to the solution surface reaction with gaseous reagent, the solid film with composition and density gradient and thickness from 100 nm to 1 μm is formed. Subsequently, after the removal of unreacted reagent excess and reaction products, the film rolls up during drying into microtubes or, in a different terminology, microscrolls with the diameter from 5 to 100 μm and length from 100 μm to 2 mm.

## 2. Experimental methods

$\text{FeCl}_2 \cdot 4\text{H}_2\text{O}$  (provided by Aldrich) and  $\text{FeCl}_3 \cdot 6\text{H}_2\text{O}$  (chemically pure, from Vekton) were used as reagents. Aqueous solutions were prepared using Milli-Q high purity water with a resistivity of more than  $18 \text{ M}\Omega/\text{cm}$ . A  $\text{FeCl}_2/\text{FeCl}_3$  mixed solution with ratio of salts of 1/2 and total concentration of 0.05 was used as the aqueous precursor. An aqueous solution of ammonium hydroxide (25 %, extra pure, from Vekton) served as the source of gaseous  $\text{NH}_3$ . The synthesis procedure was as follows: 4 mL of the mixed salt solution was poured into a flat vessel and added to a glass-lined  $50 \text{ cm}^3$  chemical reactor. Next, 2 mL of  $\text{NH}_4\text{OH}$  solution was poured into a second vessel and put in reactor near the solution vessel. The treatment lasted from 0.5 to 10 min. The thin brownish-black transparent film was formed on the solution surface during the treatment. After that, the film was twice transferred to the surface of distilled water in order to remove excess of reagent solution for 5 minutes. After washing, the film was transferred to the surface of a Teflon wafer and then dried at room temperature for 5 hours. During drying, the thin solid film was transformed into microtubes (microscrolls). Characterization of microtubes was carried out by X-ray diffraction (XRD), Scanning electron microscopy (SEM), electron probe microanalysis (EPMA). X-ray powder diffraction was performed on a Rigaku Miniflex II diffractometer. The measurement conditions were  $\text{Cu K}\alpha$  radiation, 30 kV, and 10 mA. The morphology of microtube sample was determined using scanning electron microscopy (Zeiss EVO-40EP or Merlin). The chemical composition of the samples was controlled by EDX analysis using a scanning electron microscope equipped with an INCA 350 Energy EDX analyzer (Oxford Instruments). The magnetic properties of the microtubes samples were investigated by a Lake Shore 7410 vibrating sample magnetometer at room temperature.

## 3. Results

When the surface of an aqueous  $\text{FeCl}_2$  and  $\text{FeCl}_3$  solution is exposed to gaseous ammonia, a brownish-black transparent thin solid film with thickness from 0.5 to  $1.5 \mu\text{m}$ , depending on the time of treatment, is formed. As a result of air drying at room temperature, thin solid film, acquired by the treatment during 30 seconds, transforms into the microtubes with diameter from 5 to  $10 \mu\text{m}$  and length of 80–120  $\mu\text{m}$  (Fig. 1(a,b)). The thin films synthesized with a shorter processing time are mechanically unstable. The thick films synthesized with a longer treatment time do not form a microtubule structure, apparently because they have thickness of more than  $1 \mu\text{m}$ . Therefore, mechanical strains arising during drying are not enough to bend them into the microtubes. The microtube wall consists of nanoparticles with diameter about 10 nm (Fig. 1(c)). According to the EPMA results (not reported here), the tubes consist of Fe and O atoms. Furthermore, no Cl and N atoms, which could possibly build the composition of microtubes from the solution or gaseous reagent, are detected in the sample.

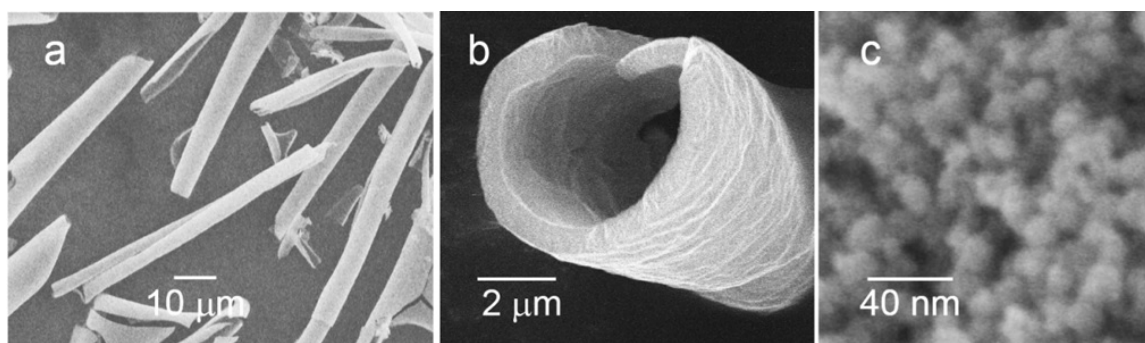
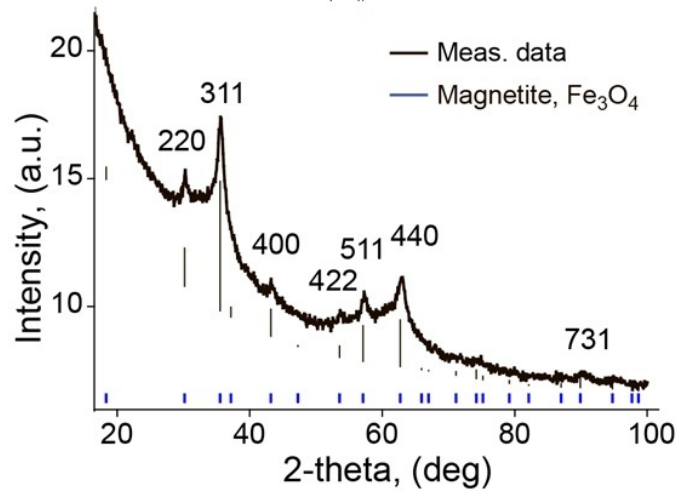
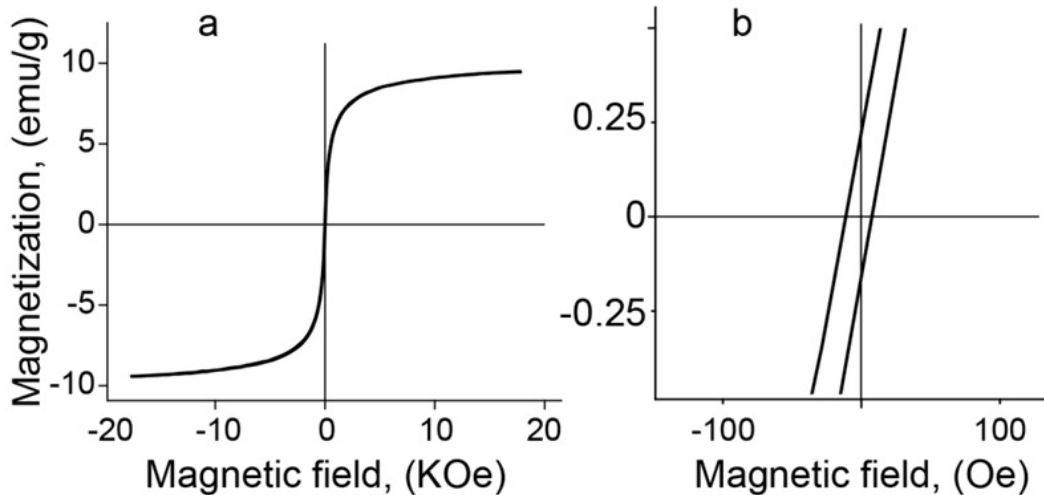


FIG. 1. SEM images of the  $\text{Fe}_3\text{O}_4$  microtubes: a) general view; b) cross view of a single microtube; c) view on the surface of microtube wall

Figure 2 shows the XRD patterns of synthesized microtubes. One can see a series of diffraction peaks at  $2\theta = 30.1, 35.4, 43.0, 53.4, 56.9, 62.5$  and so on related to the  $\text{Fe}_3\text{O}_4$  with  $Fd-3m$  space group (JCPDS card 01-080-6403).

Vibrating sample magnetometer analysis was used to investigate the magnetic behavior of the formed  $\text{Fe}_3\text{O}_4$  microtubes. The magnetic data obtained from the as-prepared microtubes of  $\text{Fe}_3\text{O}_4$  is presented in Fig. 3. Fig. 3(a) shows the hysteresis loop  $M(H)$  of the  $\text{Fe}_3\text{O}_4$  microtubes at room temperature from  $-20 \text{ kOe}$  to  $20 \text{ kOe}$ . The Fig. 3(b) shows the magnified hysteresis loop around the zero field. The saturation magnetization value is  $9.5 \text{ emu/g}$ , remanence magnetization value is  $0.2 \text{ emu/g}$ , coercive force is  $8.1 \text{ Oe}$ , and  $M_r/M_s = 0.02$ . These parameters indicate the synthesized microtubes have a superparamagnetic nature.

FIG. 2. XRD patterns of as-synthesized  $\text{Fe}_3\text{O}_4$  microtubesFIG. 3. Magnetization curves of as-synthesized  $\text{Fe}_3\text{O}_4$  microtubes: a) magnetic hysteresis loop at room temperature; b) details around zero field

#### 4. Discussion

When analyzing the experimental results, attention is primarily drawn to the fact that the obtained saturation magnetization value of 9.5 emu/g is several times smaller than the value characteristic for  $\text{Fe}_3\text{O}_4$  nanoparticles. Apparently, this value can be explained by the fact that the microtubule wall contains both water-solvent molecules, that did not completely evaporate upon room temperature air-drying, as well as amorphous  $\text{Fe}(\text{OH})_3$  hydroxide, which could form at the interface between the solution of  $\text{FeCl}_2$ - $\text{FeCl}_3$  salts mixture and gaseous ammonia at the first moment of treatment. Objectively, as it follows from the dependences of solubility logarithms of  $\text{Fe}(\text{II})$  and  $\text{Fe}(\text{III})$  hydroxides from the solution pH, calculated by Hydra-Medusa program [25], when the pH is increased in such a solution, precipitation of  $\text{Fe}(\text{OH})_3$  is observed on the first stage and then, precipitate of  $\text{Fe}(\text{OH})_2$  is formed at a pH of 7.5–12 (Fig. 4). According to the results of [26], the formation of  $\text{Fe}_3\text{O}_4$  nanoparticles in the process of precipitation of  $\text{FeCl}_2$ - $\text{FeCl}_3$  salts mixture is observed in the pH range of about 11–12. Consequently, one can assume that during synthesis, under gaseous ammonia treatment,  $\text{Fe}(\text{OH})_3$  nanoparticles are formed on the solution surface and only after that  $\text{Fe}_3\text{O}_4$  nanoparticles emerge. In our view, this effect provides composition anisotropy along the thickness of the growing film, which ultimately leads to the appearance of a density gradient and mechanical forces distorting the flat geometry of the thin film as result of drying. It is known that effect of the film composition on geometrical parameters of tubular structures was found for nanoscrolls, obtained using hydrothermal synthesis conditions [27,28].

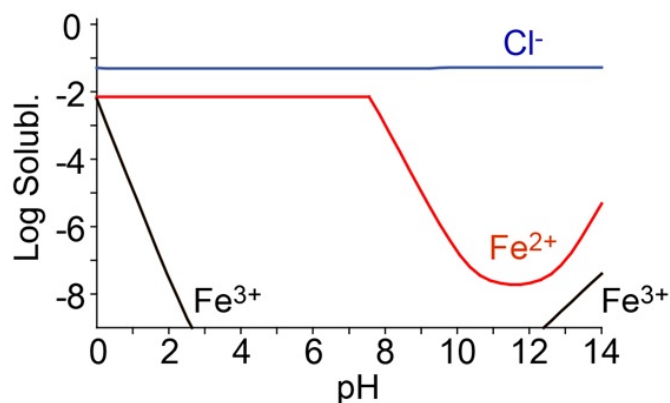


FIG. 4. Logarithms of solubility vs pH of  $\text{FeCl}_2/\text{FeCl}_3$  mixed solution.  $C_{(\text{FeCl}_2)} = 0.017 \text{ M}$ ,  $C_{(\text{FeCl}_3)} = 0.033 \text{ M}$

## 5. Conclusion

For the first time ever, a facile interface-mediated synthesis method for the fabrication of microtubes, containing  $\text{Fe}_3\text{O}_4$  nanoparticles, in the absence of catalysts or templates under soft chemistry conditions has been developed. As a result of the interaction between the mixed aqueous solution of Fe(II) and Fe(III) salts with gaseous phase ammonia a solid film is formed on the surface of the solution. During air-drying at room temperature the thin film was transformed into microtubes with diameters approximately 5–10  $\mu\text{m}$  and up to 120  $\mu\text{m}$  long with walls 0.6  $\mu\text{m}$  thick. SEM, EPMA and XRD analyzes established that the microtubes contain  $\text{Fe}_3\text{O}_4$  nanoparticles. The low coercive force and remanence magnetization, approaching of  $M_r/M_s$  to zero and the reversible hysteresis behavior confirm the superparamagnetic nature of the microtubes. The effect of film “rolling up” occurs due to the film composition gradient along its thickness, which when the film is dried, leads to the appearance of forces that distort its planar geometry and results in the formation of a more stable microtubular structure.

## Acknowledgments

This work was supported by the Russian Science Foundation (project No. 16-13-10223). We thank the Centre for X-ray Diffraction Studies and Centre for Innovative Technologies of Composite Nanomaterials of Saint Petersburg State University for their technical assistance with the investigation of the synthesized product.

## References

- [1] Hong-Ying Su, Chang-Qiang Wu, Dan-Yang Li, Hua Ai. Self-assembled superparamagnetic nanoparticles as MRI contrast agents. A review. *Chinese Physics B*, 2015, **24**, P. 127506.
- [2] Lomanova N.A., Gusarov V.V. Influence of synthesis temperature on  $\text{BiFeO}_3$  nanoparticle formation. *Nanosystems: Physics, Chemistry, Mathematics*, 2013, **4**(5), P. 696–705.
- [3] Almjasheva O.V., Gusarov V.V. Prenucleation formations in control over synthesis of  $\text{CoFe}_2\text{O}_4$  nanocrystalline powders. *Russ. J. Appl. Chem.*, 2016, **89**, P. 851–855.
- [4] Popkov V.I., Almjasheva O.V. Formation mechanism of  $\text{YFeO}_3$  nanoparticle under the hydrothermal conditions. *Nanosystems: Physics, Chemistry, Mathematics*, 2014, **5**(5), P. 703–708.
- [5] Tugova E.A., Zvereva I.A. Formation mechanism of  $\text{GdFeO}_3$  nanoparticles under the hydrothermal conditions. *Nanosystems: Physics, Chemistry, Mathematics*, 2013, **4**(6), P. 851–856.
- [6] Zherebtsov D.A., Mirasov V.Sh., Kleschev D.G., Polyakov E.V. Nanodisperse oxide compounds of iron formed in the  $\text{FeSO}_4\text{-KOH-H}_2\text{O-H}_2\text{O}_2$  system (4.0 pH 13.0). *Nanosystems: Physics, Chemistry, Mathematics*, 2015, **6**(4), P. 593–604.
- [7] Lomanova N.A., Tomkovich M.V., Sokolov V.V., Gusarov V.V. Special Features of Formation of Nanocrystalline  $\text{BiFeO}_3$  via the Glycine-Nitrate Combustion Method. *Russian Journal of General Chemistry*, 2016, **86**(10), P. 2256–2262.
- [8] Lomanova N.A., Pleshakov I.V., Volkov M.P., Gusarov V.V. Magnetic properties of Aurivillius phases  $\text{Bi}_{m+1}\text{Fe}_{m-3}\text{Ti}_3\text{O}_{3m+3}$  with  $m = 5, 7, 8$ . *Materials Science and Engineering: B*, 2016, **214**, P. 51–56.
- [9] Yang C., Wu J., and Hou Y.  $\text{Fe}_3\text{O}_4$  nanostructures: synthesis, growth mechanism, properties and applications. *Chemical Communications*, 2011, **47**(18), P. 5130–5141.
- [10] Kuklo L.I., Tolstoy V.P. Successive ionic layer deposition of  $\text{Fe}_3\text{O}_4@\text{H}_x\text{MoO}_4 \cdot n\text{H}_2\text{O}$  composite nanolayers and their superparamagnetic properties. *Nanosystems: Physics, Chemistry, Mathematics*, 2016, **7**(6), P. 1050–1054.
- [11] Hudson R. Coupling the magnetic and heat dissipative properties of  $\text{Fe}_3\text{O}_4$  particles to enable applications in catalysis, drug delivery, tissue destruction and remote biological interfacing. *RSC Advances*, 2016, **6**, P. 4262–4270.
- [12] Massart R. Preparation of aqueous magnetic liquids in alkaline and acidic media. *IEEE Transactions on Magnetics*, 1981, **17**(2), P. 1247–1248.

- [13] Qian G., Aiwu Zh., Hongyan G. et al. Controlled synthesis of Au- $Fe_3O_4$  hybrid hollow spheres with excellent SERS activity and catalytic properties. *Dalton Transactions*, 2014, **43**, P. 7998–8006.
- [14] Shan J., Wang L., Yu H., Ji J., Amer W. A., Chen Y., Jing G., Khalid H., Akram M., Abbasi N. M. Recent progress in  $Fe_3O_4$  based magnetic nanoparticles: from synthesis to application. *Materials Science and Technology*, 2016, **32**(6), P. 602–614.
- [15] Chao X., Xiaolong L., Honglian D. The Synthesis of Size-Adjustable Superparamagnetism  $Fe_3O_4$  Hollow Microspheres. *Nanoscale Research Letters*, 2017, **12**, P. 234.
- [16] Fei-Xiang M., Han H., Hao Bin W., Cheng-Yan X., Zhichuan X., Liang Zh., Xiong W. Lou. Formation of Uniform  $Fe_3O_4$  Hollow Spheres Organized by Ultrathin Nanosheets and Their Excellent Lithium Storage Properties. *Advanced Materials*, 2015, **27**, P. 4097–4101.
- [17] Goswami M.M., Dey Ch., Bandyopadhyay A., Sarkar D., Ahir M. Micelles-driven magnetite ( $Fe_3O_4$ ) hollow spheres and a study on AC magnetic properties for hyperthermia application. *Journal of Magnetism and Magnetic Materials*, 2016, **417**, P. 376–381.
- [18] Wei D., Lin Hu, Zhigao Sh. et al. Magneto-acceleration of Ostwald ripening in hollow  $Fe_3O_4$  nanospheres. *CrystEngComm*, 2016, **18**, P. 6134.
- [19] Tolstoy V.P., Gulina L.B. New way of  $As_2S_3$  microtubules preparation by roll up thin films synthesized at the air-solution interface. *Journal of Nano- and Electronic Physics*, 2013, **5**(1), P. 01003-1-01003-3.
- [20] Tolstoy V.P., Gulina L.B. Synthesis of birnessite structure layers at the solution-air interface and the formation of microtubules from them. *Langmuir*, 2014, **30**(28), P. 8366–8372.
- [21] Tolstoy V.P., Gulina L.B. Ozone interaction with manganese acetate solution. Formation of  $H_xMnO_2 \cdot nH_2O$  layers and microtubes based on them. *Russian Journal of General Chemistry*, 2013, **83**(9), P. 1635-1639.
- [22] Gulina L.B., Schäfer M., Privalov A.F., Tolstoy V.P., Murin I.V., Vogel M. Synthesis and NMR investigation of 2D nanocrystals of the  $LaF_3$  doped by  $SrF_2$ . *Journal of Fluorine Chemistry*, 2016, **188**, P. 185–190.
- [23] Gulina L.B., Tolstoy V.P., Kasatkin I.A., Petrov Y.V. Facile synthesis of  $LaF_3$  strained 2D nanoparticles and microtubes at solution-gas interface. *Journal of Fluorine Chemistry*, 2015, **180**, P. 117–121.
- [24] Gulina L.B., Tolstoy V.P. Reaction of gaseous hydrogen fluoride with the surface of lanthanum chloride solution to form  $LaF_3 \cdot nH_2O$  film and microtubes thereof. *Russian Journal of General Chemistry*, 2014, **84**(8), P. 1472–1475.
- [25] Semishchenko K., Tolstoy V., Lobinsky A. A Novel Oxidation-Reduction Route for Layer-by-Layer Synthesis of  $TiO_2$  Nanolayers and Investigation of Its Photocatalytic Properties. *Journal of Nanomaterials*, 2014, Article ID 632068, 7 pp.
- [26] Kang Y.S., Risbud S., Rabolt J.F. and Stroeve P. Synthesis and Characterization of Nanometer-Size  $Fe_3O_4$  and  $\gamma-Fe_2O_3$  Particles. *Chemistry of Materials*, 1996, **8**(9), P. 2209–2211.
- [27] Krasilin A.A., Suprun A.M., Ubyivovk E.V., Gusarov V.V. Morphology vs. chemical composition of single Ni-doped hydrosilicate nanoscroll, *Materials Letters*, 2016, **171**, P. 68–71.
- [28] Krasilin A.A., Gusarov V.V. Control over morphology of magnesium-aluminum hydrosilicate nanoscrolls, *Russian Journal of Applied Chemistry*, 2015, **88**(12), P. 1928–1935.